bioRxiv preprint doi: https://doi.org/10.1101/2020.01.23.917666; this version posted January 24, 2020. The copyright holder for this preprint (which was not certified by peer review) is the author/funder, who has granted bioRxiv a license to display the preprint in perpetuity. It is made available under aCC-BY-NC-ND 4.0 International license.

# Enhancing $CO_2$-valorization using *Clostridium autoethanogenum* for sustainable fuel and chemicals production

1 **James K. Heffernan[1&], Kaspar Valgepea[1,2&], Renato de Souza Pinto Lemgruber[1],**
2 **Isabella Casini[3], Manuel Plan[4], Ryan Tappel[5], Sean D. Simpson[5], Michael Köpke[5],**
3 **Lars K. Nielsen[1,4], Esteban Marcellin[1,4*]**

4 [1]Australian Institute for Bioengineering and Nanotechnology, The University of
5 Queensland, Building 75, Corner College Rd & Cooper Rd, St. Lucia 4067, QLD,
6 Australia.

7 [2]ERA Chair in Gas Fermentation Technologies, Institute of Technology, University of
8 Tartu, Nooruse 1, 50411 Tartu, Estonia.

9 [3]Center for Applied Geosciences, University of Tübingen, Hölderlinstr. 12, 72074,
10 Tübingen, Germany.

11 [4]Queensland Node of Metabolomics Australia, The University of Queensland, Building
12 75, Corner College Rd & Cooper Rd, St. Lucia 4067, QLD, Australia.

13 [5]LanzaTech Inc., 8045 Lamon Ave Suite 400, Skokie, IL 60077, USA.

14 *** Correspondence:**
15 Corresponding author
16 e.marcellin@uq.edu.au

17 **[&] Equal contributors**

18 **Keywords: gas fermentation, *Clostridium autoethanogenum*, carbon dioxide,**
19 **valorization, carbon recycling, fuel and chemical platforms.**

20 **Abstract**

21 Acetogenic bacteria can convert waste gases into fuels and chemicals. Design of
22 bioprocesses for waste carbon valorization requires quantification of steady-state carbon
23 flows. Here, steady-state quantification of autotrophic chemostats containing
24 *Clostridium autoethanogenum* grown on $CO_2$ and $H_2$ revealed that captured carbon (460
25 ± 80 mmol/gDCW/day) had a significant distribution to ethanol (54 ± 3 mol% with a
26 2.4 ± 0.3 g/L titer). We were impressed with this initial result, but also observed
27 limitations to biomass concentration and growth rate. Metabolic modelling predicted
28 culture performance and indicated significant metabolic adjustments when compared to
29 fermentation with CO as the carbon source. Moreover, modelling highlighted flux to
30 pyruvate, and subsequently reduced ferredoxin, as a target for improving $CO_2$ and $H_2$
31 fermentation. Supplementation with a small amount of CO enabled co-utilisation with
32 $CO_2$, and enhanced $CO_2$ fermentation performance significantly, while maintaining an
33 industrially relevant product profile. Additionally, the highest specific flux through the
34 Wood-Ljungdahl pathway was observed during co-utilization of $CO_2$ and CO.

bioRxiv preprint doi: https://doi.org/10.1101/2020.01.23.917666; this version posted January 24, 2020. The copyright holder for this preprint (which was not certified by peer review) is the author/funder, who has granted bioRxiv a license to display the preprint in perpetuity. It is made available under aCC-BY-NC-ND 4.0 International license.



35 Furthermore, the addition of CO led to superior $CO_2$-valorizing characteristics (9.7 ±
36 0.4 g/L ethanol with a 66 ± 2 mol% distribution, and 540 ± 20 mmol $CO_2$/gDCW/day).
37 Similar industrial processes are commercial or currently being scaled up, indicating CO-
38 supplemented $CO_2$ and $H_2$ fermentation has high potential for sustainable fuel and
39 chemical production. This work also provides a reference dataset to advance our
40 understanding of $CO_2$ gas fermentation, which can contribute to mitigating climate
41 change.

## 42 Introduction

43 Gas fermentation has attractive waste carbon valorization properties, for which the need
44 is intensifying (Emerson and Stephanopoulos, 2019; IPCC, 2014). Recently, LanzaTech
45 commercialized the first waste gas-to-ethanol process, efficiently incorporating the
46 carbon from steel mill off-gas into fuel quality ethanol *via* the model acetogen
47 *Clostridium autoethanogenum*. The key carbon source — carbon monoxide (CO) —
48 accounts for a significant portion of steel mill off-gas and synthesis gas (syngas), which
49 can be generated from multiple high-volume, non-gaseous waste feedstocks (e.g.
50 biomass, municipal solid waste) (Liew et al., 2016). Therefore, LanzaTech's process is
51 significant in that it valorizes waste carbon by fusing two one-carbon gas molecules
52 (C1) into liquid fuel. Furthermore, Handler et al. (2016) found that ethanol produced by
53 LanzaTech's process reduced greenhouse gas emissions by 67 to 98% when compared
54 to petroleum gasoline on an energy content and "cradle-to-grave" basis (feedstock
55 dependent). Carbon dioxide ($CO_2$) represents a more diverse and plentiful waste stream
56 compared to CO (International Panel on Climate Change (IPCC), 2014), thus
57 embodying a feedstock with greater climate change mitigation and carbon recycling
58 potential.

59 Increasing acetogenic carbon capture as $CO_2$ would build on the success of commercial
60 gas fermentation and continue the expansion of the technology as a platform for
61 sustainable chemical production (Bengelsdorf et al., 2018; Müller, 2019; Redl et al.,
62 2017). Compared to other $CO_2$ valorization methods, acetogens are ideal candidates due
63 to their high metabolic efficiency, ability to handle variable gas compositions, high
64 product specificity, scalability, and low susceptibility to poisoning by sulphur, chlorine,
65 and tars (Artz et al., 2018; Liew et al., 2016). However, metabolism of $CO_2$ requires an
66 energy source, for which some see an appropriate solution is lacking (Emerson and
67 Stephanopoulos, 2019).

68 Gas fermenting acetogens harbor the Wood-Ljungdahl pathway (WLP) (Drake et al.,
69 2008), a non-photosynthetic C1-fixation metabolic pathway with the highest-known
70 theoretical thermodynamic efficiency (Fast and Papoutsakis, 2012; Müller, 2019;
71 Schuchmann and Müller, 2014). Various potential energy sources exist for metabolizing
72 $CO_2$, primarily hydrogen, nitrates, sugars, and arginine. Yet, acetogenic $CO_2$
73 valorization, which is actively being developed for industrial implementation (Tizard
74 and Sechrist, 2015), poses challenges along with promise. These include potential
75 adenosine triphosphate (ATP) starvation in autotrophic conditions and carbon catabolite
76 repression in hetero/mixotrophic conditions (Emerson and Stephanopoulos, 2019).

77 Hydrogen ($H_2$) is the most recognized energy source for $CO_2$ utilization — as
78 metabolism of sugars or nitrates cause shifts in metabolism that result in lower $CO_2$ or

bioRxiv preprint doi: https://doi.org/10.1101/2020.01.23.917666; this version posted January 24, 2020. The copyright holder for this preprint (which was not certified by peer review) is the author/funder, who has granted bioRxiv a license to display the preprint in perpetuity. It is made available under aCC-BY-NC-ND 4.0 International license.



79 $H_2$ utilization (Emerson and Stephanopoulos, 2019 & Liew et al., 2016). $H_2$ production
80 will also logically transition to renewable sources in the future, whereas production of
81 sugars and nitrates are dependent on less-sustainable methods. Furthermore, levelized
82 cost predictions for solar $H_2$ indicate a 30% reduction by 2030, potentially becoming
83 competitive with the current levelized cost of fossil fuel derived $H_2$ by 2035 (Detz et al.,
84 2018; Glenk and Reichelstein, 2019). This is in part due to rapidly decreasing solar
85 electricity costs (IRENA, 2017) and projections of $H_2$ electrolysis technology
86 development (Detz et al., 2018; Glenk and Reichelstein, 2019). Similarly, atmospheric
87 $CO_2$ capture *via* direct air contact showed promising feasibility recently (Keith et al.,
88 2018), which represents an essential development for carbon recycling (Otto et al.,
89 2015). Various power-to-gas technologies are being discussed for mediating
90 fluctuations in renewable power generation (Götz et al., 2016). By extension, gas
91 fermentation to liquid products could couple mediation of renewable power fluctuations
92 to carbon recycling (Redl et al., 2017). This provides an attractive new opportunity for
93 bacterial artificial-photosynthesis, whereby renewable $H_2$ supplementation facilitates
94 acetogenic $CO_2$ valorization (Claassens et al., 2016; Haas et al., 2018).

95 Continuous culture bioprocesses are preferable to batch or fed-batch fermentation
96 bioprocesses (Hoskisson and Hobbs, 2005). Furthermore, systems-level quantification is
97 essential for design-build-test-learn bioprocess optimization by metabolic engineering
98 (Valgepea et al., 2017). Therefore, obtaining quantitative datasets from steady-state
99 chemostat cultures, whose analyses are comparable between experiments, is important
100 for development of these systems (Adamberg et al., 2015). Whilst Bengelsdorf et al.
101 (2018) reviewed autotrophic acetogen growth on $CO_2$ and $H_2$ ($CO_2$+$H_2$), and Mock et
102 al. (2015) provided notable insight into the $CO_2$+$H_2$ metabolism of *C.*
103 *autoethanogenum*, the literature lacks a steady-state dataset where carbon flows in a
104 $CO_2$+$H_2$ fermentation are quantified. Here we aimed to quantify steady-state $CO_2$+$H_2$
105 fermentation using fully instrumented chemostats and the model acetogen *C.*
106 *autoethanogenum*. Subsequently, we showed that $CO_2$ is a promising feedstock
107 alternative to CO, as more than half of the substrate $CO_2$ carbon was converted into
108 ethanol. Furthermore, supplementation with CO at low concentrations improved
109 fermentation performance significantly.

110 **Materials and Methods**

111 **Bacterial strain, growth medium, and continuous culture conditions**

112 A derivate of *Clostridium autoethanogenum* DSM 10061 strain—DSM 19630—
113 deposited in the German Collection of Microorganisms and Cell Cultures (DSMZ) was
114 used in all experiments and stored as glycerol stocks at − 80 °C. This non-commercial
115 strain was grown on $CO_2$+$H_2$ (~23% $CO_2$, ~67% $H_2$ and ~10% Ar; BOC Australia) and
116 CO/$CO_2$/$H_2$ (~2% CO, ~23% $CO_2$, ~65% $H_2$, and ~10% Ar; BOC Australia) in
117 chemically defined medium (Valgepea et al., 2017). Cells were grown under strictly
118 anaerobic conditions at 37 °C and at a pH of 5 (maintained by 5 M $NH_4OH$). Chemostat
119 continuous culture achieved steady-states at dilution rates (D) = 0.47 ± 0.01 ($CO_2$+$H_2$;
120 specific growth rate (μ) = 0.0196 ± 0.0004 [average ± standard deviation]), 0.5 ± 0.01,
121 and 1 ± 0.01 day$^{-1}$ (CO/$CO_2$/$H_2$; μ = 0.021 ± 0.0004, and 0.042 ± 0.0008 h$^{-1}$
122 respectively). See Table 1 for steady-state gas-liquid mass transfer rate data. The steady-
123 state results reported here were collected after optical density (OD), gas uptake and

bioRxiv preprint doi: https://doi.org/10.1101/2020.01.23.917666; this version posted January 24, 2020. The copyright holder for this preprint (which was not certified by peer review) is the author/funder, who has granted bioRxiv a license to display the preprint in perpetuity. It is made available under aCC-BY-NC-ND 4.0 International license.



124 production rates had been stable in chemostat mode for at least three working volumes.
125 See Valgepea et al. (2017a) for details on equipment.

## 126 Experimental analysis

### 127 Biomass concentration and extracellular metabolome analyses

128 Biomass concentration (gDCW/L) was estimated and extracellular metabolome analysis
129 carried out as specified in Valgepea et al. (2018).

### 130 Bioreactor off-gas analysis

131 Bioreactor off-gas was analyzed by an online Hiden HPR-20-QIC mass spectrometer.
132 The Faraday Cup detector monitored the intensities of $H_2$, CO, ethanol, $H_2S$, Ar, and
133 $CO_2$ at 2, 14, 31, 34, 40, and 44 amu, respectively, in the bioreactor off-gas. These
134 masses were chosen so that each target compound would be represented by a unique
135 signal. This was determined to be essential to achieve the highest confidence in
136 quantification using preliminary experiments as interferences from other compounds at
137 a shared mass could not be reliably accounted for (e.g. the more intense signal from CO
138 at 28 amu could not be used due to the uncertainty of interference at 28 amu from the
139 $CO_2$ fragment). Gas from the cylinder was used as the calibration gas for each MS-cycle
140 (i.e. 'online calibration') to achieve reliable off-gas analysis (Valgepea et al., 2017). See
141 below for details on quantification of gas uptake and production rates.

## 142 Quantification

### 143 Gas uptake and production rates

144 Gas uptake (CO, $CO_2$ and $H_2$) and production (ethanol) were determined using "online
145 calibration" of the MS by analyzing the respective feed gas directly from the cylinder
146 after each analysis cycle of the bioreactors. Specific rates (mmol/gDCW/h) were
147 calculated by taking into account the exact composition of the respective gas, bioreactor
148 liquid working volume, feed gas flow rate, off-gas flow rate (based on the fractional
149 difference of the inert gas [Ar] in the feed and off-gas composition), the molar volume
150 of ideal gas, and the steady-state biomass concentration.

### 151 Carbon balance analysis

152 The carbon balances were determined at 116 ± 11%, 103 ± 12%, and 108 ± 11% for
153 $CO_2$+$H_2$, and CO/$CO_2$/$H_2$ at D = 0.5 and 1 $day^{-1}$ respectively (total C-mol products/total
154 C-mol substrates), as specified in Valgepea et al. (2017).

## 155 Genome-scale metabolic modelling with GEM iCLAU786

156 Model simulations were performed using genome scale model (GEM) iCLAU786 of *C.*
157 *autoethanogenum* and flux balance analysis (FBA) (Orth and Palsson, 2011) as
158 specified in Valgepea et al. (2018). Briefly, we used FBA to estimate intracellular fluxes
159 (SIM1–26) and predict "optimal" growth phenotypes for experimental conditions
160 (SIM27–62) using either maximization of ATP dissipation or biomass yield,
161 respectively, as the objective function. Complete simulation results identified as SIMx

bioRxiv preprint doi: https://doi.org/10.1101/2020.01.23.917666; this version posted January 24, 2020. The copyright holder for this preprint (which was not certified by peer review) is the author/funder, who has granted bioRxiv a license to display the preprint in perpetuity. It is made available under aCC-BY-NC-ND 4.0 International license.



162 (e.g. SIM1) in the text are in Supplementary Files. SIM1-19, 27-41, and 49-55 are from
163 Valgepea et al. (2018). In addition to details described in Valgepea et al. (2018), $CO_2$
164 reduction to formate was forced from the formate dehydrogenase (FdhA) reaction
165 scheme (rxn00103_c0, SIM17-30) to the FdhA/Hydrogenase ABCDE complex
166 (HytABCDE) reaction scheme (rxn08518_c0, SIM31-40) when maximizing for
167 biomass formation, as described by Mock et al. (2015). SIM56-62 also stopped export
168 of pyruvate (rxn05469_c0), a decision validated by HPLC data.

## 169 Results

### 170 *Clostridium autoethanogenum* steady-state fermentation of carbon dioxide and
171 hydrogen

172 *Clostridium autoethanogenum* cells reached steady-state when growing on $CO_2$+$H_2$ in
173 chemostats at dilution rate (D) ~0.5 day$^{-1}$ (specific growth rate (μ) ~0.02 h$^{-1}$) with a
174 biomass concentration of 0.18 ± 0.02 g dry cell weight (gDCW)/L (Figure 1**A**). It is
175 important to note that attempts to reach a steady-state at D =1 day$^{-1}$ were unsuccessful.
176 Unlike the chemostat cultures of *C. autoethanogenum* with CO (Valgepea et al., 2018;
177 2017a) and $CO_2$+$H_2$ retentostat cultures (Mock et al., 2015), the $CO_2$+$H_2$ cultures could
178 not reach stable biomass concentrations before the culture began oscillation cycles;
179 previously observed above ~1.6 gDCW/L (Valgepea et al., 2017). The physiological
180 reason and mechanism for such oscillatory culture behavior are under investigation, but
181 we assumed that cell recycling is a requirement for $CO_2$+$H_2$ culture stability. For
182 example, Molitor et al. (2019) showed consistent, high-biomass concentration and high-
183 acetate $CO_2$+$H_2$ fermentation with *Clostridium ljungdahlii* in a retentostat with
184 complete recycling.

185 Despite the attempt to reach a steady-state at D = 1 day$^{-1}$, cells reached steady-state at
186 dilution rate = 0.5 day$^{-1}$. Under those conditions, the specific production rates of ethanol
187 and acetate were 140 ± 10 and 113 ± 9 mmol/gDCW/day, respectively (Figure 1**C**).
188 Strikingly, the specific rate of carbon incorporation (i.e. $qCO_2$) was 480 ± 80
189 mmol/gDCW/day (Figure 1**B**), and around half of that carbon was captured as ethanol
190 (54 ± 3 mol%) (Figure 1**D**). Fermentation conditions and titers are available in Table 1,
191 showing an impressive ethanol concentration compared to previous fermentations where
192 CO was the main carbon and energy source.

193 Despite the different dilution rate, the $CO_2$+$H_2$ results generated were compared to
194 previously published chemostat cultures of *C. autoethanogenum* grown on CO, syngas,
195 and CO+$H_2$ (Valgepea et al., 2018) at similar biomass concentrations (~0.5 gDCW/L)
196 (Figure 1**B**, **C** & **D**). Specific rates of acetate and ethanol production achieved here for
197 $CO_2$+$H_2$ cultures fell between those for syngas (■) and CO+$H_2$ (■) cultures (Figure 1**B**
198 & **D**). However, the specific rate of carbon incorporation was higher for $CO_2$+$H_2$
199 (Figure 1**C**). We found that more than half of the captured $CO_2$ was converted into
200 ethanol (Figure 1**D**). These results were encouraging, especially as ethanol production
201 has unfavorable stoichiometry compared to acetate (Mock et al., 2015). Furthermore,
202 the $H_2$ specific uptake rate (1130 ± 160 mmol/gDCW/day) showed that higher $H_2$
203 uptake rates are achievable (compared to old datasets). These results show that higher
204 carbon yields are possible (Valgepea et al., 2018). To further investigate the metabolic
205 demand and the feasibility of $CO_2$+$H_2$ fermentation, we utilized the steady-state dataset

bioRxiv preprint doi: https://doi.org/10.1101/2020.01.23.917666; this version posted January 24, 2020. The copyright holder for this preprint (which was not certified by peer review) is the author/funder, who has granted bioRxiv a license to display the preprint in perpetuity. It is made available under aCC-BY-NC-ND 4.0 International license.



206 as constraints for the GEM to find candidate mechanisms for improving $CO_2$+$H_2$
207 fermentation using iCLAU786.

## 208 Metabolic model of carbon dioxide and hydrogen fermentation

209 Estimation of intracellular processes constrained by *in vivo* datasets represents an
210 important developmental step for progressing acetogenic $CO_2$ valorization. Here, for
211 instance, comparing $CO_2$+$H_2$ and CO-containing fermentation fluxes was possible
212 (Figure 2). See Supplementary Files for complete details.

213 Intracellular metabolite fluxes from the FBA showed remarkable similarity to the
214 combined theoretical stoichiometry of acetate and ethanol production (Mock et al.,
215 2015) and indicated energetic cofactor circuits with mapping close to 1:1
216 (experimental:theoretical stoichiometry; Supplementary Files). Ethanol production
217 likely occurred *via* acetaldehyde:ferredoxin oxidoreductase (AOR; leq000004) under
218 autotrophic conditions, with the HytABCDE (leq000001) and Nfn complex (leq000002)
219 likely facilitating cofactor production *via* electron bifurcation (Figure 2) (Valgepea et
220 al., 2018). This is a mechanism for minimization of free energy loss employed by *C.*
221 *autoethanogenum* and may play a key role in sustaining proton motive force by
222 balancing acetate, ethanol, and ATP production (Mock et al., 2015; Valgepea et al.,
223 2018). Engineering acetogens to redirect this energy towards cellular growth, sacrificing
224 some ethanol production, could be beneficial for $CO_2$ fermentation (Emerson and
225 Stephanopoulos, 2019).

226 It was notable that, unlike CO fermentations, the pyruvate:ferredoxin oxidoreductase
227 (PFOR; rxn05938_c0; acetyl-CoA ↔ pyruvate) flux was not significantly in the
228 direction of pyruvate (Figure 2) (Valgepea et al., 2018). Under autotrophic conditions,
229 PFOR links the WLP to anabolic pathways associated with biomass (Furdui and
230 Ragsdale, 2000), and therefore this indicated high cell-specific energetic limitation.
231 From this observation, we hypothesized that CO supplementation could provide a
232 potential solution, as CO oxidation would generate $Fd_{red}$. Furthermore, an ATP/$H_2$ flux
233 ratio of ~0.15 was observed here compared to an ATP/CO ratio of ~0.28 in CO only
234 fermentations (Valgepea et al., 2018). Considering CO+$H_2$ and $CO_2$+$H_2$ fermentations
235 had equal carbon-flux through the WLP (~10 mmol/gDCW/h; Figure 2),
236 supplementation with renewable CO from $CO_2$ electrolysis could control biomass
237 formation and culture stability. A similar process (but CO fermentation) was detailed by
238 Haas et al. (2018).

## 239 *Clostridium autoethanogenum* steady-state fermentation of carbon dioxide and 240 hydrogen supplemented with carbon monoxide

241 To validate our modelling hypothesis, *Clostridium autoethanogenum* was cultured with
242 a low concentration of carbon monoxide in addition to $CO_2$ and $H_2$ (CO/$CO_2$/$H_2$) in
243 chemostats. A steady-state was reached at D = 0.5 day$^{-1}$ (μ ~0.02 h$^{-1}$), and at D =1 day$^{-1}$
244 (μ ~0.04 h$^{-1}$; Figure 1**A**; biomass concentrations of 0.54 ± 0.01 and 0.34 ± 0.02
245 gDCW/L respectively). CO/$CO_2$/$H_2$ fermentations at a D = 1 day$^{-1}$ (CO/$CO_2$/$H_2^{1}$) and a
246 D = 0.5 day$^{-1}$ (CO/$CO_2$/$H_2^{0.5}$) showed simultaneous uptake of CO (89 ± 2 and 36 ± 4
247 mmol/gDCW/day, respectively) and $CO_2$ (940 ± 20 and 540 ± 20 mmol/gDCW/day,
248 respectively) (Figure 1**B**). The co-utilization of both C1 gases is, to the best of our

bioRxiv preprint doi: https://doi.org/10.1101/2020.01.23.917666; this version posted January 24, 2020. The copyright holder for this preprint (which was not certified by peer review) is the author/funder, who has granted bioRxiv a license to display the preprint in perpetuity. It is made available under aCC-BY-NC-ND 4.0 International license.



249 knowledge, an unquantified phenomenon. This led to a specific carbon incorporation
250 ($CO/CO_2/H_2^1$ – 1030 ± 30 mmol/gDCW/day) larger than any other gas type (maximum
251 of ~450 mmol/gDCW/day for fermentations with CO in Valgepea et al. (2018) or
252 $CO_2$+$H_2$ in this work). This also resulted in significant improvements to culture
253 performance compared to $CO_2$+$H_2$ fermentations.

254 Compared to $CO_2$+$H_2$, $CO/CO_2/H_2^{0.5}$ showed higher acetate and ethanol titers (Table 1)
255 and specific productivities (Figure 1**C**), and a higher ethanol/acetate ratio (2.15 vs 1.24
256 mol/mol respectively). While at a similar biomass concentration ($CO/CO_2/H_2^1$ best
257 comparison due to similarity in dilution rate), acetate and ethanol titers (Table 1), and
258 specific productivities (Figure 1**C**) are greater than during fermentation of other CO-
259 containing gases. When comparing to high biomass (~1.4 gDCW/L) CO cultures, CO-
260 supplementation still performs impressively – CO+$H_2$ fermentation achieved a higher
261 ethanol titer (11.6 ± 0.4 g/L), while CO and syngas fermentations were similar (3.9 ±
262 0.2 and 5.4 ± 0.3 g/L respectively). Otherwise, all specific productivities were higher for
263 $CO/CO_2/H_2^1$ (Supplementary Files). Furthermore, the distribution of carbon to ethanol
264 was still greater than 50% (Figure 1**D**; 53.8 ± 0.4 % and 66 ± 2% for $CO/CO_2/H_2^1$ and
265 $CO/CO_2/H_2^{0.5}$ respectively).

266 To understand the metabolic effects of supplementing CO, FBA was performed using
267 the same conditions and alterations as for $CO_2$+$H_2$ (Figure 2). Notably, the WLP
268 specific flux throughput for $CO/CO_2/H_2^1$ was ~2-fold greater than for any other gas type
269 (including high-biomass [Valgepea et al., 2018]). Furthermore, for $CO_2$ fermentations,
270 Nfn complex flux direction was opposite that of CO and syngas fermentations.
271 $CO/CO_2/H_2^{0.5}$ also showed significantly greater flux through the AOR, whilst specific
272 WLP productivity was insignificantly different compared to $CO_2$+$H_2$.

273 **Discussion**

274 Achieving steady-state continuous cultures using $CO_2$+$H_2$ mixtures, without cell
275 recycling here, was challenging. Yet, compared to other organisms fermenting $CO_2$+$H_2$
276 with continuous medium exchange, *Clostridium autoethanogenum* performs well (Table
277 2). No direct comparisons can be made to other experiments due to variations in
278 conditions, but *C. autoethanogenum* clearly achieves the highest ethanol production,
279 with comparable quantities of carbonous products also. *Acetobacterium woodii*, along
280 with *Sporomusa ovata*, were shown to perform well when compared to a wide range of
281 acetogens under batch $CO_2$+$H_2$ conditions (Groher and Weuster-Botz, 2016). Yet, as
282 evidenced by omission of *S. ovata* from Table 2, few continuous culture
283 characterizations of acetogens are available – an essential step for validation of
284 industrial robustness in gas fermentation. As discussed by Molitor et al. (2019), the lack
285 of yeast extract or $C_{\geq 2}$ substrates is also distinguishing between fermentations.

286 Notably, $CO_2$+$H_2$ cultures displayed higher variability between biological replicates
287 compared to those of CO-containing gas mixtures (Figure 1) (Valgepea et al., 2017).
288 This may indicate variable organism fitness, a trait previously discussed for *C.*
289 *autoethanogenum* by Liew et al. (2016), who extensively covered numerous techniques
290 used for enhancing gas fermentation including – coupling to other processes, adaptive
291 laboratory evolution, and metabolic engineering of acetogens using genetic tools. CO-
292 supplementation could be a valuable option for enhancement as it overcomes inherent

bioRxiv preprint doi: https://doi.org/10.1101/2020.01.23.917666; this version posted January 24, 2020. The copyright holder for this preprint (which was not certified by peer review) is the author/funder, who has granted bioRxiv a license to display the preprint in perpetuity. It is made available under aCC-BY-NC-ND 4.0 International license.



293 problems linked to engineering acetogens. Supplementation of low quantities of CO
294 here stabilized the culture, enabled culturing at D =1 $day^{-1}$, and achieved higher biomass
295 concentration with a carbon incorporation larger than any other gas type – all without
296 compromising by-product distribution.

297 While Valgepea et al. (2018) found that syngas fermentation lead to CO-only
298 fermentation at steady-state, we observed co-utilization of CO and $CO_2$. Tizard and
299 Sechrist (2015) have also shown co-utilization for *C. autoethanogenum* continuous
300 cultures, and it seems that co-uptake may also occur for some points of syngas batch
301 fermentation ([preprint] Infantes et al., 2020). Co-utilization of sugars was found for *E.*
302 *coli* in chemostats – where inhibition of consumption, but no change in induction time
303 was observed (Standing et al., 1972). The WLP is most likely no different, in that
304 metabolism of CO is preferential, yet the pathway can co-consume $CO_2$ under certain
305 conditions.

306 Various efforts have been made towards enhancing $CO_2(+H_2)$ fermentation to $C_{\geq 2}$
307 products (Table 2) (Emerson and Stephanopoulos, 2019). Braun and Gottschalk (1981)
308 first discovered the potential for enhancement when *Acetobacterium woodii*
309 simultaneously consumed fructose and a headspace of $CO_2$+$H_2$ during batch cultivation.
310 Growth and acetate production was high but no characterization of the headspace was
311 performed. More recently, continuous glucose-supplemented $CO_2$+$H_2$ fermentation of
312 *Moorella thermoacetica* by Park et al. (2019) did not lead to net uptake of $CO_2$.
313 Furthermore, Jones et al. (2016) did not show net $CO_2$ uptake for a wide range of
314 acetogens (not *A. woodii*) fermenting syngas and fructose. *A. woodii* generates a sodium
315 ion ($Na^+$) gradient (Hess et al., 2013) rather than a proton ($H^+$) gradient for membranous
316 ATP generation (Bengelsdorf et al., 2018; Pierce et al., 2008; Poehlein et al., 2015).
317 This may highlight an important metabolic difference from other model acetogens –
318 decoupling the resources of the WLP and membranous ATP generation pathways could
319 facilitate fermentation of sugar and $CO_2$+$H_2$ simultaneously.

320 Other enhancements have also struggled to achieve net $CO_2$ uptake. Co-culture of *C.*
321 *acetobutylicum* and *C. ljungdahlii* showed syntrophic metabolic coupling when
322 fermenting glucose, fructose, and $CO_2$+$H_2$, but no net $CO_2$ uptake (Charubin and
323 Papoutsakis, 2019). Addition of nitrate to batch $CO_2$+$H_2$ fermentation by *C. ljungdahlii*,
324 increased biomass concentration and subsequently volumetric productivity of acetate
325 (Emerson et al., 2019). However, the specific WLP productivity decreased, meaning
326 lower utilization of $CO_2$. Other organisms not recognized as gas fermenters can also use
327 mixotrophy to minimize carbon loss, such as *Clostridium beijerinckii* but have not
328 displayed net $CO_2$ uptake either (Sandoval-Espinola et al., 2017). To the best of our
329 knowledge, this is the first report where supplementation of a substrate other than $H_2$,
330 increased productivities of continuous acetogenic $CO_2$ fermentation while maintaining
331 net $CO_2$ utilization. Furthermore, the effect of CO supplementation on $CO_2$ utilization
332 was superlinear, indicating a synergistic mechanism (Park et al., 2019). This is
333 encouraging for development of bioprocesses valorizing $CO_2$.

334 Comparisons between fermentation datasets enables us to speculate about the positive
335 effect of CO-supplementation on $CO_2$+$H_2$ fermentation. Although, addition of CO led to
336 minimal metabolic shifts (Figure 2 – $CO_2$+$H_2$ vs $CO/CO_2/H_2^{0.5}$ and Supplementary
337 Files), FBA showed that CO supplementation caused significant increases to the

bioRxiv preprint doi: https://doi.org/10.1101/2020.01.23.917666; this version posted January 24, 2020. The copyright holder for this preprint (which was not certified by peer review) is the author/funder, who has granted bioRxiv a license to display the preprint in perpetuity. It is made available under aCC-BY-NC-ND 4.0 International license.



338 reduced ferredoxin consumption by AOR and Rnf complex (leq000004 and M002,
339 respectively) compared to $CO_2$+$H_2$ (Figure 2). The overflow model proposed by Richter
340 et al. (2016) suggests that high NADH production *via* Rnf and Nfn complexes
341 (leq000002) is also important for reducing AOR product inhibition. In this way, NADH
342 facilitates fast metabolism of acetaldehyde to ethanol *via* alcohol dehydrogenase
343 (Adh(E); rxn00543_c0). Decreasing the acetate concentration reduces acidification and
344 the ATP cost for excreting acetate (Valgepea et al., 2018). Including acetaldehyde
345 conversion to ethanol and association to acetic acid, this also leads to consumption of 2
346 $H^+$ (4 here vs 2 produced *via* CODH). Therefore, CO consumption decreases the
347 intracellular $H^+$ pool, and following Le Chatelier's principle, drives HytABCDE
348 activity. Indeed, the change in specific $H_2$ uptake relative to specific $CO_2$ uptake is
349 greater than that of CO (for $CO_2$+$H_2$ vs CO/$CO_2$/$H_2$ at D = 0.5 $day^{-1}$, Supplementary
350 Files). Subsequently, the relative gain in free energy from $H_2$ is ~ 4-fold greater than
351 CO. We speculate this is ultimately responsible for the improved fitness of CO-
352 supplemented $CO_2$+$H_2$ fermentation by *C. autoethanogenum*. We propose the following
353 five critical factors to this enhanced metabolism: [1] metabolism of CO increases the
354 intracellular pool of reduced ferredoxin; [2] this stimulates oxidation of ferredoxin,
355 which if consumed by the AOR; [3] reduces ATP costs; and [4] decreases the $H^+$
356 pool/acidification; which therefore [5] drives $H_2$ uptake for further reduction of
357 ferredoxin. Evidently, additional understanding of acetogenic redox metabolism, from a
358 thermodynamic perspective, is important for developing acetogenic $CO_2$-valorization as
359 a platform industrial bioprocess (Cueto-Rojas et al., 2015).

360 Physicochemical properties could also play a key role in CO-supplementation enabling
361 to achieve a stable $CO_2$+$H_2$ chemostat culture at D =1 $day^{-1}$. Generation of a stable and
362 large non-equilibrium is what drives microbial growth (Igamberdiev and Kleczkowski,
363 2009; Qian and Beard, 2005; Quéméner and Bouchez, 2014) and gas-liquid mass
364 transfer (Ma et al., 2005). For continuous culture of gas fermenting microbes, an
365 inherent relationship between substrate mass transfer and culture growth exists
366 (Supplementary Files). An important parameter for these systems is the Gibb's free
367 energy of a system (Cueto-Rojas et al., 2015). This describes the thermodynamic
368 favorability of the reaction system – termed spontaneity. Here, analysis of experimental
369 flux and Gibbs free energy suggests that $CO_2$+$H_2$ fermentation is infeasible ($\Delta\dot{G}^0_{OR} =$
370 $5.4\ kJ/mol/day$), whereas CO-supplemented $CO_2$+$H_2$ fermentation is feasible
371 ($\Delta\dot{G}^0_{OR} = -12.3\ kJ/mol/day$; Supplementary Files). Though these calculations use
372 standard conditions, they do indicate how close $CO_2$+$H_2$ fermentation is to the
373 thermodynamic limit of metabolism. Theoretically, minute and unobservable changes to
374 chemostat $CO_2$+$H_2$ fermentation can disrupt the culture (Henry and Martin, 2016).
375 Thus, increasing the free energy of central metabolism with CO-supplementation
376 appears to keep metabolism in a spontaneous and stable state by increasing reduced
377 ferredoxin production.

378 The mechanisms for achieving the 2-fold higher specific WLP flux throughput for
379 CO/$CO_2$/$H_2$[1] compared to others is less clear but appears to be linked to the difference
380 in primary substrate. CO/$CO_2$/$H_2$[1] and CO+$H_2$ are the most similar $CO_2$ and CO
381 fermentations, respectively (D ~1 $day^{-1}$ and carbon to hydrogen feed ratio (~1:3); Table
382 1), and the maximum carbon incorporation per cell for CO+$H_2$ was roughly half of that
383 of CO/$CO_2$/$H_2$[1] (~450 vs ~1000 mmol/gDCW). Theoretically, cells will maximize

bioRxiv preprint doi: https://doi.org/10.1101/2020.01.23.917666; this version posted January 24, 2020. The copyright holder for this preprint (which was not certified by peer review) is the author/funder, who has granted bioRxiv a license to display the preprint in perpetuity. It is made available under aCC-BY-NC-ND 4.0 International license.



384 carbon-to-redox metabolism by minimizing thermodynamic losses. CO supplementation
385 to a $CO_2$+$H_2$ culture seems to facilitate this as $(H_2/carbon)_{feed} – (H_2/carbon)_{flux}$ was ~0
386 mol/mol for CO/$CO_2$/$H_2$ fermentations only (Supplementary Files) – an indication of
387 the relative magnitude of carbon and redox metabolism. This suggests that high specific
388 fluxes for CO/$CO_2$/$H_2$[1] may be a result of (close to) optimal co-factor recycling by *C.*
389 *autoethanogenum*'s WLP and redox pathway. Thus, the lower energy associated with
390 $CO_2$ fermentation may, counterintuitively, stimulate specific WLP activity when in the
391 presence of appropriate energy-containing substrates. Further quantifications of $CO_2$
392 metabolism and characterizations of enzyme activities are required to confirm these
393 hypotheses (Supplementary Files), as they assist our ability to engineer the links
394 between redox and carbon metabolisms.

395 We established a dataset quantifying steady-state of the model acetogen *C.*
396 *autoethanogenum* during autotrophic-$CO_2$+$H_2$ growth in chemostat cultures. This
397 enabled analysis *via* FBA, and highlighted CO as a potential supplement. CO
398 supplementation successfully improved metabolic stability and $CO_2$ utilization. This
399 was the first time that intracellular fluxes for net uptake of $CO_2$ (with enhancement)
400 where characterized. Industry is actively developing gas fermentation to valorize $CO_2$
401 (Haas et al., 2018 & Tizard and Sechrist, 2015). Previously, genetic and process
402 engineering of gas fermentation successfully developed the technology for industrial
403 CO valorization (Liew et al., 2016). Therefore, progression to industrial $CO_2$
404 valorization is foreseeable, and CO supplementation may play a role in the continuing
405 diversification of industrial gas fermentation.

406 **Conflict of Interest**

407 The authors declare that this study received funding from the Australian Research
408 Council (ARC), partly funded by LanzaTech (ARC LP140100213). The ARC had no
409 involvement with the study. LanzaTech has interest in commercializing gas
410 fermentation with *C. autoethanogenum*. RT, SDS and MK are employees of LanzaTech.

411 **Author Contributions**

412 All authors viewed and approved the manuscript. All authors contributed significantly
413 to the work. KV, EM, and LN conceived the project. JH, KV and EM designed the
414 experiments and analysed the results. JH and KV performed experiments, supported by
415 RL, IC, MP, and EM. JH wrote the manuscript with the help of KV, EM, RT, SS, MK,
416 and LN.

417 **Funding**

418 This study was funded by a Grant from the Australian Research Council, partly funded
419 by LanzaTech (ARC LP140100213).

420 **Acknowledgments**

421 Elements of this research utilized equipment and support provided by the Queensland
422 node of Metabolomics Australia, an initiative of the Australian Government being
423 conducted as part of the NCRIS National Research Infrastructure for Australia. IC

bioRxiv preprint doi: https://doi.org/10.1101/2020.01.23.917666; this version posted January 24, 2020. The copyright holder for this preprint (which was not certified by peer review) is the author/funder, who has granted bioRxiv a license to display the preprint in perpetuity. It is made available under aCC-BY-NC-ND 4.0 International license.



424 would like to acknowledge support from the German Academic Exchange Service
425 (DAAD) through the "DAAD Kurzstipendien für Doktoranden". We thank the
426 following investors in LanzaTech's technology: Sir Stephen Tindall, Khosla Ventures,
427 Qiming Venture Partners, Softbank China, the Malaysian Life Sciences Capital Fund,
428 Mitsui, Primetals, CICC Growth Capital Fund I, L.P. and the New Zealand
429 Superannuation Fund. There was no funding support from the European Union for the
430 experimental part of the study. However, KV acknowledges support also from the
431 European Union's Horizon 2020 research and innovation programme under grant
432 agreement N810755.

## 433 Contribution to the field

434 Acetogenic bacteria comprise an ancient lineage and play a major role in global carbon
435 cycle (accounting for at least $10^{13}$ kg of acetate produced annually and 20% of the fixed
436 carbon on earth). Due to their ability to grow autotrophically on carbonous waste-gas
437 feedstocks, these organisms have gained significant interest in biotechnological
438 applications. However, acetogens are considered living at the thermodynamic edge of
439 life when growing autotrophically. Although they have evolved sophisticated strategies
440 to conserve energy from reduction potential differences between major redox couples,
441 this coupling is sensitive to small changes in thermodynamic equilibria. In the
442 manuscript, we present experimental data showing $CO_2$ conversion to ethanol by an
443 acetogenic bacteria used for industrial scale gas fermentation. Furthermore, we showed
444 that supplementing CO enhances $CO_2$+$H_2$ fermentation performance significantly.
445 Analysis was only possible due to the first rigorously quantified dataset from
446 continuous $CO_2$ and $H_2$ fermentation. This enabled discovery of notable insights into
447 metabolic function – providing a potential guide for metabolic engineering. Therefore,
448 here we outline that *Clostridium autoethanogenum* offers a promising route for the
449 sustainable production of fuels and chemicals from a wide range of waste feedstocks –
450 including $CO_2$.

## 451 Supplementary Files

452 The Supplementary Files for this article can be found online.

## 453 References

454 Adamberg, K., Valgepea, K., and Vilu, R. (2015). Advanced continuous cultivation
455 methods for systems microbiology. *Microbiol. (United Kingdom)* 161, 1707–1719.
456 doi:10.1099/mic.0.000146.

457 Artz, J., Müller, T. E., Thenert, K., Kleinekorte, J., Meys, R., Sternberg, A., et al.
458 (2018). Sustainable Conversion of Carbon Dioxide: An Integrated Review of
459 Catalysis and Life Cycle Assessment. *Chem. Rev.* 118, 434–504.
460 doi:10.1021/acs.chemrev.7b00435.

461 Bengelsdorf, F. R., Beck, M. H., Erz, C., Hoffmeister, S., Karl, M. M., Riegler, P., et al.
462 (2018). Bacterial Anaerobic Synthesis Gas (Syngas) and CO 2 + H 2 Fermentation.
463 *Adv. Appl. Microbiol.* doi:10.1016/bs.aambs.2018.01.002.

bioRxiv preprint doi: https://doi.org/10.1101/2020.01.23.917666; this version posted January 24, 2020. The copyright holder for this preprint (which was not certified by peer review) is the author/funder, who has granted bioRxiv a license to display the preprint in perpetuity. It is made available under aCC-BY-NC-ND 4.0 International license.



464 Braun, K., and Gottschalk, G. (1981). Effect of molecular hydrogen and carbon dioxide
465 on chemo-organotrophic growth of Acetobacterium woodii and Clostridium
466 aceticum. *Arch. Microbiol.* 128, 294–298. doi:10.1007/BF00422533.

467 Charubin, K., and Papoutsakis, E. T. (2019). Direct cell-to-cell exchange of matter in a
468 synthetic Clostridium syntrophy enables CO2 fixation, superior metabolite yields,
469 and an expanded metabolic space. *Metab. Eng.* 52, 9–19.
470 doi:10.1016/j.ymben.2018.10.006.

471 Claassens, N. J., Sousa, D. Z., dos Santos, V. A. P. M., de Vos, W. M., and van der
472 Oost, J. (2016). Harnessing the power of microbial autotrophy. *Nat. Rev.*
473 *Microbiol.* 14, 692–706. doi:10.1038/nrmicro.2016.130.

474 Cueto-Rojas, H. F., van Maris, A. J. a. J. A., Wahl, S. A., and Heijnen, J. J. J. (2015).
475 Thermodynamics-based design of microbial cell factories for anaerobic product
476 formation. *Trends Biotechnol.* 33, 534–546. doi:10.1016/j.tibtech.2015.06.010.

477 Detz, R. J., Reek, J. N. H., and Van Der Zwaan, B. C. C. (2018). The future of solar
478 fuels: When could they become competitive? *Energy Environ. Sci.* 11, 1653–1669.
479 doi:10.1039/c8ee00111a.

480 Drake, H. L., Gößner, A. S., and Daniel, S. L. (2008). Old acetogens, new light. *Ann. N.*
481 *Y. Acad. Sci.* 1125, 100–128. doi:10.1196/annals.1419.016.

482 Emerson, D. F., and Stephanopoulos, G. (2019). Limitations in converting waste gases
483 to fuels and chemicals. *Curr. Opin. Biotechnol.* 59, 39–45.
484 doi:https://doi.org/10.1016/j.copbio.2019.02.004.

485 Emerson, D. F., Woolston, B. M., Liu, N., Donnelly, M., Currie, D. H., and
486 Stephanopoulos, G. (2019). Enhancing hydrogen-dependent growth of and carbon
487 dioxide fixation by Clostridium ljungdahli through nitrate supplementation.
488 *Biotechnol. Bioeng.* 116, 294–306. doi:10.1002/bit.26847.

489 Fast, A. G., and Papoutsakis, E. T. (2012). Stoichiometric and energetic analyses of
490 non-photosynthetic CO2-fixation pathways to support synthetic biology strategies
491 for production of fuels and chemicals. *Curr. Opin. Chem. Eng.* 1, 380–395.
492 doi:10.1016/j.coche.2012.07.005.

493 Furdui, C., and Ragsdale, S. W. (2000). The role of pyruvate ferredoxin oxidoreductase
494 in pyruvate synthesis during autotrophic growth by the Wood-Ljungdahl pathway.
495 *J. Biol. Chem.* 275, 28494–28499. doi:10.1074/jbc.M003291200.

496 Glenk, G., and Reichelstein, S. (2019). Economics of converting renewable power to
497 hydrogen. *Nat. Energy* 4. doi:10.1038/s41560-019-0326-1.

498 Götz, M., Lefebvre, J., Mörs, F., McDaniel Koch, A., Graf, F., Bajohr, S., et al. (2016).
499 Renewable Power-to-Gas: A technological and economic review. *Renew. Energy*
500 85, 1371–1390. doi:10.1016/j.renene.2015.07.066.

501 Groher, A., and Weuster-Botz, D. (2016). Comparative reaction engineering analysis of

bioRxiv preprint doi: https://doi.org/10.1101/2020.01.23.917666; this version posted January 24, 2020. The copyright holder for this preprint (which was not certified by peer review) is the author/funder, who has granted bioRxiv a license to display the preprint in perpetuity. It is made available under aCC-BY-NC-ND 4.0 International license.



502 different acetogenic bacteria for gas fermentation. *J. Biotechnol.* 228, 82–94.
503 doi:10.1016/j.jbiotec.2016.04.032.

504 Haas, T., Krause, R., Weber, R., Demler, M., and Schmid, G. (2018). Technical
505 photosynthesis involving CO2 electrolysis and fermentation. *Nat. Catal.* 1, 32–39.
506 doi:10.1038/s41929-017-0005-1.

507 Handler, R. M., Shonnard, D. R., Griffing, E. M., Lai, A., and Palou-Rivera, I. (2016).
508 Life Cycle Assessments of Ethanol Production via Gas Fermentation: Anticipated
509 Greenhouse Gas Emissions for Cellulosic and Waste Gas Feedstocks. *Ind. Eng.*
510 *Chem. Res.* 55, 3253–3261. doi:10.1021/acs.iecr.5b03215.

511 Henry, A., and Martin, O. C. (2016). Short relaxation times but long transient times in
512 both simple and complex reaction networks. *J. R. Soc. Interface*.
513 doi:https://doi.org/10.1098/rsif.2016.0388.

514 Hess, V., Schuchmann, K., and Müller, V. (2013). The ferredoxin: NAD+
515 Oxidoreductase (Rnf) from the acetogen acetobacterium woodii requires na+ and is
516 reversibly coupled to the membrane potential. *J. Biol. Chem.* 288, 31496–31502.
517 doi:10.1074/jbc.M113.510255.

518 Hoffmeister, S., Gerdom, M., Bengelsdorf, F. R., Linder, S., Flüchter, S., Öztürk, H., et
519 al. (2016). Acetone production with metabolically engineered strains of
520 Acetobacterium woodii. *Metab. Eng.* 36, 37–47. doi:10.1016/j.ymben.2016.03.001.

521 Hoskisson, P. A., and Hobbs, G. (2005). Continuous culture - Making a comeback?
522 *Microbiology* 151, 3153–3159. doi:10.1099/mic.0.27924-0.

523 Hu, P., Chakraborty, S., Kumar, A., Woolston, B. M., Liu, H., Emerson, D., et al.
524 (2016). Integrated Bioprocess for Conversion of Gaseous Substrates to Liquids.
525 *Proc. Natl. Acad. Sci.* 113, 2–7. doi:10.1073/pnas.1516867113.

526 Igamberdiev, A. U., and Kleczkowski, L. A. (2009). Metabolic systems maintain stable
527 non-equilibrium via thermodynamic buffering. *BioEssays* 31, 1091–1099.
528 doi:10.1002/bies.200900057.

529 Infantes, A., Kugel, M., and Neumann, A. (2020). Effect of Cysteine , Yeast Extract ,
530 pH Regulation and Gas Flow on Acetate and Ethanol Formation and Growth
531 Profiles of Clostridium ljungdahlii Syngas Fermentation. *bioRxiv [preprint]*.
532 doi:http://dx.doi.org/10.1101/2020.01.13.904292.

533 International Panel on Climate Change (IPCC) (2014). *Climate Change 2014:*
534 *Mitigation of Climate Change*. doi:10.1017/CBO9781107415416.

535 IRENA (2017). Renewable Power Generation Costs in 2017.
536 doi:10.1007/SpringerReference_7300.

537 Jones, S. W., Fast, A. G., Carlson, E. D., Wiedel, C. A., Au, J., Antoniewicz, M. R., et
538 al. (2016). CO 2 fixation by anaerobic non-photosynthetic mixotrophy for
539 improved carbon conversion. *Nat. Commun.* 7, 1–9. doi:10.1038/ncomms12800.

bioRxiv preprint doi: https://doi.org/10.1101/2020.01.23.917666; this version posted January 24, 2020. The copyright holder for this preprint (which was not certified by peer review) is the author/funder, who has granted bioRxiv a license to display the preprint in perpetuity. It is made available under aCC-BY-NC-ND 4.0 International license.



540 Kantzow, C., Mayer, A., and Weuster-Botz, D. (2015). Continuous gas fermentation by
541 Acetobacterium woodii in a submerged membrane reactor with full cell retention.
542 *J. Biotechnol.* 212, 11–18. doi:10.1016/j.jbiotec.2015.07.020.

543 Keith, D. W., Holmes, G., St. Angelo, D., and Heidel, K. (2018). A Process for
544 Capturing CO2 from the Atmosphere. *Joule* 2, 1573–1594.
545 doi:10.1016/J.JOULE.2018.05.006.

546 Klask, C., Kliem-kuster, N., Molitor, B., and Angenent, L. T. (2019). An open-source
547 multiple-bioreactor system for replicable gas- fermentation experiments : Nitrate
548 feed results in stochastic inhibition events , but improves ethanol production of
549 Clostridium ljungdahlii with CO 2 and H 2. *bioRxiv [preprint]*.
550 doi:https://doi.org/10.1101/2019.12.15.877050.

551 Liew, F. M., Martin, E., Tappel, R., Heijstra, B., Mihalcea, C., and Köpke, M. (2016).
552 Gas Fermentation – A Flexible Platform for Commercial Scale Production of Low
553 Carbon Fuels and Chemicals from Waste and Renewable Feedstocks. *Front.*
554 *Microbiol.* 7, 694. doi:10.3389/fmicb.2016.00694.

555 Ma, Y., Yu, G., and Li, H. Z. (2005). Note on the mechanism of interfacial mass
556 transfer of absorption processes. *Int. J. Heat Mass Transf.* 48, 3454–3460.
557 doi:10.1016/j.ijheatmasstransfer.2005.03.008.

558 Mock, J., Zheng, Y., Mueller, A. P., Ly, S., Tran, L., Segovia, S., et al. (2015). Energy
559 conservation associated with ethanol formation from H2and CO2in Clostridium
560 autoethanogenum involving electron bifurcation. *J. Bacteriol.*
561 doi:10.1128/JB.00399-15.

562 Molitor, B., Mishra, A., and Angenent, L. T. (2019). Power-to-protein: converting
563 renewable electric power and carbon dioxide into single cell protein with a two-
564 stage bioprocess. *Energy Environ. Sci.* doi:10.1039/C9EE02381J.

565 Morinaga, T., and Kawada, N. (1990). The production of acetic acid from carbon
566 dioxide and hydrogen by an anaerobic bacterium. *J. Biotechnol.* 14, 187–194.
567 doi:10.1007/BF02146190.

568 Müller, V. (2019). New Horizons in Acetogenic Conversion of One-Carbon Substrates
569 and Biological Hydrogen Storage. *Trends Biotechnol.* 37, 1344–1354.
570 doi:10.1016/j.tibtech.2019.05.008.

571 Orth, J. D., and Palsson, B. Ø. (2011). What is flux balance analysis? *Nat. Biotechnol.*
572 28, 245–248. doi:10.1038/nbt.1614.What.

573 Otto, A., Grube, T., Schiebahn, S., and Stolten, D. (2015). Closing the loop: Captured
574 CO2 as a feedstock in the chemical industry. *Energy Environ. Sci.* 8, 3283–3297.
575 doi:10.1039/c5ee02591e.

576 Park, J. O., Liu, N., Holinski, K. M., Emerson, D. F., Qiao, K., Woolston, B. M., et al.
577 (2019). Synergistic substrate cofeeding stimulates reductive metabolism. *Nat.*
578 *Metab.* 1, 643–651. doi:10.1038/s42255-019-0077-0.

bioRxiv preprint doi: https://doi.org/10.1101/2020.01.23.917666; this version posted January 24, 2020. The copyright holder for this preprint (which was not certified by peer review) is the author/funder, who has granted bioRxiv a license to display the preprint in perpetuity. It is made available under aCC-BY-NC-ND 4.0 International license.




579 Pierce, E., Xie, G., Barabote, R. D., Saunders, E., Han, C. S., Detter, J. C., et al. (2008).
580 The complete genome sequence of Moorella thermoacetica (f. Clostridium
581 thermoaceticum). *Environ. Microbiol.* 10, 2550–2573. doi:10.1111/j.1462-
582 2920.2008.01679.x.

583 Poehlein, A., Cebulla, M., Ilg, M. M., Bengelsdorf, F. R., Schiel-bengelsdorf, B.,
584 Whited, G., et al. (2015). The Complete Genome Sequence of *Clostridium*
585 *aceticum*: a Missing Link between Rnf- and Cytochrome-Containing Autotrophic
586 Acetogens. *MBio* 6, e01168-15. doi:10.1128/mBio.01168-15.Editor.

587 Qian, H., and Beard, D. A. (2005). Thermodynamics of stoichiometric biochemical
588 networks in living systems far from equilibrium. *Biophys. Chem.* 114, 213–220.
589 doi:https://doi.org/10.1016/j.bpc.2004.12.001.

590 Quéméner, E. D. Le, and Bouchez, T. (2014). A thermodynamic theory of microbial
591 growth. *ISME J.* 8, 1747–1751. doi:10.1038/ismej.2014.7.

592 Redl, S., Diender, M., Jensen, T. Ø., Sousa, D. Z., and Nielsen, A. T. (2017). Exploiting
593 the potential of gas fermentation. *Ind. Crops Prod.*
594 doi:10.1016/j.indcrop.2016.11.015.

595 Richter, H., Molitor, B., Wei, H., Chen, W., Aristilde, L., and Angenent, L. T. (2016).
596 Ethanol production in syngas-fermenting Clostridium ljungdahlii is controlled by
597 thermodynamics rather than by enzyme expression. *Energy Environ. Sci.*
598 doi:10.1039/C6EE01108J.

599 Sakai, S., Nakashimada, Y., Inokuma, K., Kita, M., Okada, H., and Nishio, N. (2005).
600 Acetate and ethanol production from H2 and CO2 by Moorella sp. using a repeated
601 batch culture. *J. Biosci. Bioeng.* 99, 252–8. doi:10.1263/jbb.99.252.

602 Sandoval-Espinola, W. J., Chinn, M. S., Thon, M. R., and Bruno-Bárcena, J. M. (2017).
603 Evidence of mixotrophic carbon-capture by n-butanol-producer Clostridium
604 beijerinckii. *Sci. Rep.* 7, 1–13. doi:10.1038/s41598-017-12962-8.

605 Schuchmann, K., and Müller, V. (2014). Autotrophy at the thermodynamic limit of life:
606 a model for energy conservation in acetogenic bacteria. *Nat. Rev. Microbiol.* 12,
607 809–821. doi:10.1038/nrmicro3365.

608 Standing, C. N., Fredrickson, A. G., and Tsuchiya, H. M. (1972). Batch- and
609 continuous-culture transients for two substrate systems. *Appl. Microbiol.* 23, 354–
610 359.

611 Tizard, J. H., and Sechrist, P. A. (2015). Carbon Capture in Fermentation. U.S. Patent
612 No 0,111,266. Washington, DC: U.S. Patent and Trademark Office. Available at:
613 https://patents.justia.com/patent/20150111266.

614 Valgepea, K., De Souza Pinto Lemgruber, R., Abdalla, T., Binos, S., Takemori, N.,
615 Takemori, A., et al. (2018). H2 drives metabolic rearrangements in gas-fermenting
616 Clostridium autoethanogenum. *Biotechnol. Biofuels* 11, 55. doi:10.1186/s13068-
617 018-1052-9.

bioRxiv preprint doi: https://doi.org/10.1101/2020.01.23.917666; this version posted January 24, 2020. The copyright holder for this preprint (which was not certified by peer review) is the author/funder, who has granted bioRxiv a license to display the preprint in perpetuity. It is made available under aCC-BY-NC-ND 4.0 International license.



618 Valgepea, K., de Souza Pinto Lemgruber, R., Meaghan, K., Palfreyman, R. W.,
619 Abdalla, T., Heijstra, B. D., et al. (2017). Maintenance of ATP Homeostasis
620 Triggers Metabolic Shifts in Gas-Fermenting Acetogens. *Cell Syst.* 4.

621 **Figure captions**

622 **Figure 1.** Important fermentation characteristics of *Clostridium autoethanogenum* in
623 autotrophic chemostats. Results from Valgepea et al. (2018) are also displayed (**B**, **C** &
624 **D**), the conditions of all fermentations are summarized in Table 1. Growth curves of
625 novel fermentations with standard deviation at steady-state (**A**). Specific rates of uptake
626 (**B**) and production (**C**) for important metabolites. Product carbon balances (**D**). Values
627 represent the average ± standard deviation between biological replicates. Number of
628 biological replicates, and detailed gas composition for each fermentation are available in
629 Table 1. Patterned bars indicate a D of 1 $day^{-1}$, full bars indicate a D of 0.5 $day^{-1}$ (**B**, **C**
630 & **D**). Abbreviations: *q* –specific rate, *DCW* – dry cell weight.

631 **Figure 2.** Predictions of central metabolic pathway fluxes for autotrophic fermentations
632 of *Clostridium autoethanogenum* using iCLAU786, flux balance analysis, and
633 chemostat data. Results from Valgepea et al. (2018) are also displayed, the conditions of
634 these fermentations are summarized in Table 1. Fluxes (mmol/gDCW/h) are represented
635 as the average ± standard deviation between biological replicates. Number of biological
636 replicates, and detailed gas composition for each fermentation are available in Table 1.
637 Arrows show the direction of calculated fluxes; red arrows denote uptake or secretion,
638 dashed arrows denote a series of reactions. Brackets denote metabolites bound by an
639 enzyme. Refer to Supplementary Files for enzyme involvement, metabolite
640 abbreviations, and complete flux balance analysis datasets.

641

bioRxiv preprint doi: https://doi.org/10.1101/2020.01.23.917666; this version posted January 24, 2020. The copyright holder for this preprint (which was not certified by peer review) is the author/funder, who has granted bioRxiv a license to display the preprint in perpetuity. It is made available under aCC-BY-NC-ND 4.0 International license.



642 **Tables and Figures**

643 **Table 1.** Summary of low-biomass *Clostridium autoethanogenum* fermentations.

644

| Gas | y | F | N | BR | D | BC | | Ace | | EtOH | |
|---|---|---|---|---|---|---|---|---|---|---|---|
| | (Ar to 100%) | mL /min | rpm | # | day$^{-1}$ | gDCW /L | ± | g/L | ± | g/L | ± |
| CO | 60% CO | 50 | 510 | 4 | 1 | 0.47 | 0.02 | 2.12 | 0.18 | 0.63 | 0.05 |
| Syngas | 50 % CO, 20% $CO_2$, 20% $H_2$ | 50 | 500 | 2 | 1 | 0.48 | 0.04 | 4.35 | 0.12 | 0.61 | 0.06 |
| CO+$H_2$ | 15% CO, 45% $H_2$ | 50 | 650 | 4 | 1 | 0.46 | 0.04 | 0.69 | 0.07 | 4.46 | 0.41 |
| CO/$CO_2$/$H_2$ | 2% CO, 23% $CO_2$, 65% $H_2$ | 30 | 1200 | 2 | 1 | 0.34 | 0.02 | 5.03 | 0.34 | 4.79 | 0.43 |
| $CO_2$+$H_2$ | 23% $CO_2$, 67% $H_2$ | 32 | 500 | 3 | 0.5 | 0.18 | 0.02 | 2.51 | 0.42 | 2.36 | 0.25 |
| CO/$CO_2$/$H_2$ | 2% CO, 23% $CO_2$, 65% $H_2$ | 30 | 800 | 2 | 0.5 | 0.54 | 0.01 | 5.97 | 0.98 | 9.69 | 0.39 |

645

646 The horizontal line through the middle of the table indicates where the data is from;
647 above the line is data from (Valgepea et al., 2018), and below the line is novel data.

648 Abbreviations: y – gas compositions, F – gas flowrate, N – stirrer speed, BR –
649 biological replicates, D – dilution rate, BC – biomass concentration, Ace – acetate
650 concentration, EtOH – ethanol concentration, ± - plus/minus standard deviation.

651

bioRxiv preprint doi: https://doi.org/10.1101/2020.01.23.917666; this version posted January 24, 2020. The copyright holder for this preprint (which was not certified by peer review) is the author/funder, who has granted bioRxiv a license to display the preprint in perpetuity. It is made available under aCC-BY-NC-ND 4.0 International license.



652 **Table 2.** Summary of quantitative and continuous $CO_2$+$H_2$ fermentations.

653

| Organism | Strain | Experimental Conditions | Growth rate ($day^{-1}$) | $C_{Product}$ g[DCW]/L | Productivity g/L/day, (g/gDCW/day) | Ref. |
|---|---|---|---|---|---|---|
| *Acetobacterium woodii* | DSM 1030 | **1 L chemostat, D = 0.84 $day^{-1}$, 1200 rpm, 30 L/h 17% $CO_2$, 40% $H_2$, 43% N2, 1 atm, pH 7.0, 30 °C, 4 g/L YE, n = 1** | **μ = 0.84** | **B = 1.1<br>A = 22.0** | **A = 19.1 (17.4)** | 1 |
| | | 1 L batch retentostat, D = 1.68 $day^{-1}$, 1200 rpm, 30 L/h 17% $CO_2$, 40% $H_2$, 43% N2, 1 atm, pH 7.0, 30 °C, 4 g/L YE, n = 1 | | B = 6.0[a,b]<br>A = 22.6 | A = 40 (16.0[a,b]) | 1 |
| | | D = 4.2 $day^{-1}$ | | B = 10.0[a,b]<br>A = 23.5 | A = 95 (18.5[a,b]) | |
| | | 1 L batch retentostat, D = 8.4 $day^{-1}$, 1200 rpm, 30 L/h 25% $CO_2$, 60% $H_2$, 15% N2, 1 atm, pH 7.0, 30 °C, 4 g/L YE, n = 1 | | B = 11.0<br>A = 17.6 | A = 148 (20.3) | 1[b,c] |
| | pMTL84151 _act$_{thlA}$ | 0.85 L batch retentostat, D = 1 $day^{-1}$, 800 rpm, 30 L/h 20% $CO_2$ & 80% $H_2$, pH 7.0, 30 °C, 2 g/L YE, 10 g/L K-acetate, n = 1 | μ = 0 | B = 4.6[d]<br>A = 48.6<br>Ac = 3.0 | Ac = 0.6 (0.1) | 2 |
| *Acetobacterium* sp. | BR446 | Semi-batch retentostat, D = 24 $day^{-1}$, $CO_2$ & $H_2$, medium not specified | | B = 4.8<br>A = 3.0 | A = 71.0 (14.7) | 3 |
| *Clostridium autoethanogenum* | DSM 19630 | **0.75 L chemostat, D = 0.5 $day^{-1}$, 500 rpm, 1.92 L/h 23% $CO_2$, 67% $H_2$, 10% Ar, 1 atm, pH 5, 37 °C, DM, n = 3** | **μ = 0.5** | **B = 0.2<br>A = 2.5<br>E = 2.4** | **B = 0.1<br>A = 1.3 (6.8)<br>E = 1.2 (6.4)** | Here |
| | | **800 rpm, 1.8 L/h 2% CO, 23% $CO_2$, 67% $H_2$, 10% Ar, n = 2** | **μ = 0.5** | **B = 0.5<br>A = 6.0<br>E = 9.7** | **B = 0.3<br>A = 3.0 (5.5)<br>E = 6.3 (11.6)** | |
| | | **D = 1 $day^{-1}$, 1200 rpm** | **μ = 1.0** | **B = 0.3<br>A = 5.0<br>E = 4.8** | **B = 0.3<br>A = 5.0 (14.6)<br>E = 6.2 (18.1)** | |
| | DSM 10061 | 1.3 L continuous retentostat, D = 4.9 $day^{-1}$, 21 L/h 23% $CO_2$, 65% $H_2$, 9.2% $N_2$, pH 5.3, 37 °C, DM, 3.1 g/L ammonium acetate, n = 1 | μ = 0.5 | B = 1.8<br>A = 7.5<br>E = 6.3 | A = 36.7 (20.0)<br>E = 30.9 (16.9) | 4 |
| *Clostridium ljungdahlii* | DSM 13528 | **0.5 L chemostat, D = 0.29 $day^{-1}$, 300 rpm, 1.8 L/h 20% $CO_2$ & 80% $H_2$, pH 5.5, 37 °C, DM, n = 3** | **μ = 0.29** | **B = 0.2[e]<br>A = 6.3<br>E = 1.8** | **A = 1.8<br>E = 0.5** | 5 |
| | | **DM with $NaNO_3$ replacing $NH_4Cl$, n = 1** | **μ = 0.29** | **B = 0.3[b,e] (pH 5.5)<br>A = 13.4[b] (pH 6.0)<br>E = 5.0[b] (pH 5.0)** | **A = 3.9<br>E = 1.4** | |
| | | 1 L batch retentostat, D = 0.96 $day^{-1}$, 300 rpm, 7.2 L/h 20% $CO_2$ & 80% $H_2$, pH 5.7, 35 °C, DM, n = 1 | μ = 0 | B = 2.3[a]<br>A = 18.5 | A = 17.7 | 6 |
| *Moorella thermoacetica* | ATCC 49707 | 1 L BCR, D = 2.16 $day^{-1}$, 72 L/h 33% $CO_2$ & 67% $H_2$, pH = 6.0, 60 °C, 10 g/L YE, n = 1 | μ = 0 | B = 4.1[a]<br>A = 25.0[a] | A = 54.0 (13.3)[f] | 7 |
| *Moorella* sp. | HUC22-1 | 0.5 L semi-continuous with cell retention, 500 rpm, continuous 20% $CO_2$ & 80% $H_2$, 3.6 L/h, pH 6.2, 55 °C, 1 g/L YE, n =1 | μ = 0 | B = 1.5<br>A = 22.0<br>E = 0.3 | A = 6.9 (10.4) | 8 |

654

bioRxiv preprint doi: https://doi.org/10.1101/2020.01.23.917666; this version posted January 24, 2020. The copyright holder for this preprint (which was not certified by peer review) is the author/funder, who has granted bioRxiv a license to display the preprint in perpetuity. It is made available under aCC-BY-NC-ND 4.0 International license.



655 Thick boarders separate organisms, while thin borders separate similar experiments –
656 for which only differences in conditions are stated following the first experiment.
657 Bolded experiments are chemostats. Only biomass concentration is given in gDCW/L.

658 Ref. 1 – 8: Kantzow et al., 2015; Hoffmeister et al., 2016; Morinaga and Kawada, 1990;
659 Mock et al., 2015; (preprint) Klask et al., 2019; Molitor et al., 2019; Hu et al., 2016;
660 Sakai et al., 2005.

661 Abbreviations: $c_{Product}$ – product concentration, D - dilution rate, YE – yeast extract, DM
662 – defined medium, n – number of replicates, B – biomass, A – acetate, E – ethanol, Ac –
663 acetone, BCR – bubble column reactor.

664 Notes: [a] estimated from graph, [b] not steady state (represented as maximum), [c] cell
665 retention membrane was blocked before steady state was reached, [d] calculated using
666 data from Kantzow et al. (2015), [e] calculated using data from Molitor et al. (2019), [f]
667 calculated using estimated data.

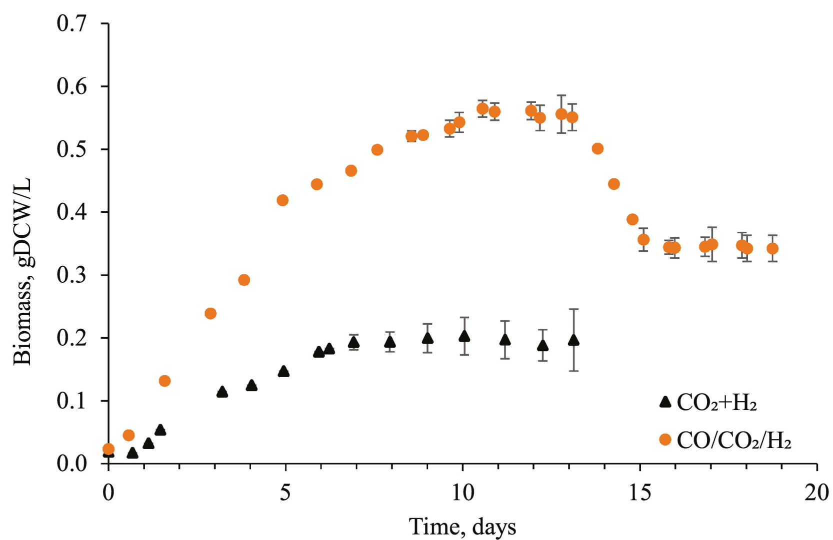
Biomass, gDCW/L
Time, days
CO₂+H₂
CO/CO₂/H₂

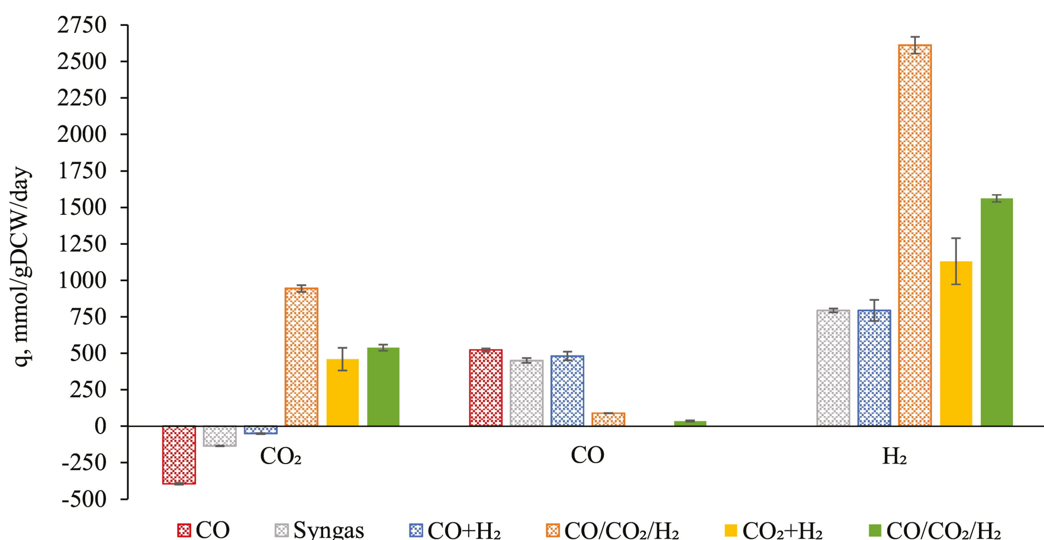
q, mmol/gDCW/day
CO₂
CO
H₂
CO
Syngas
CO+H₂
CO/CO₂/H₂
CO₂+H₂
CO/CO₂/H₂

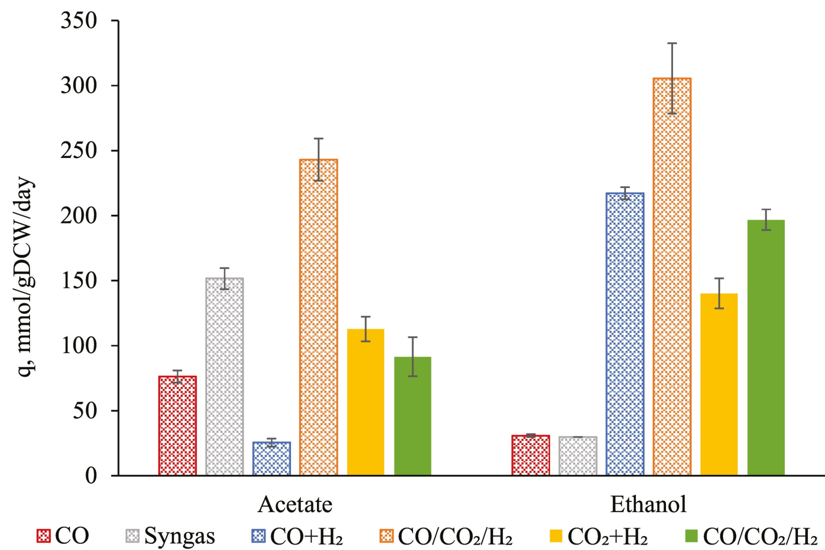
q, mmol/gDCW/day
Acetate
Ethanol
CO
Syngas
CO+H₂
CO/CO₂/H₂
CO₂+H₂
CO/CO₂/H₂

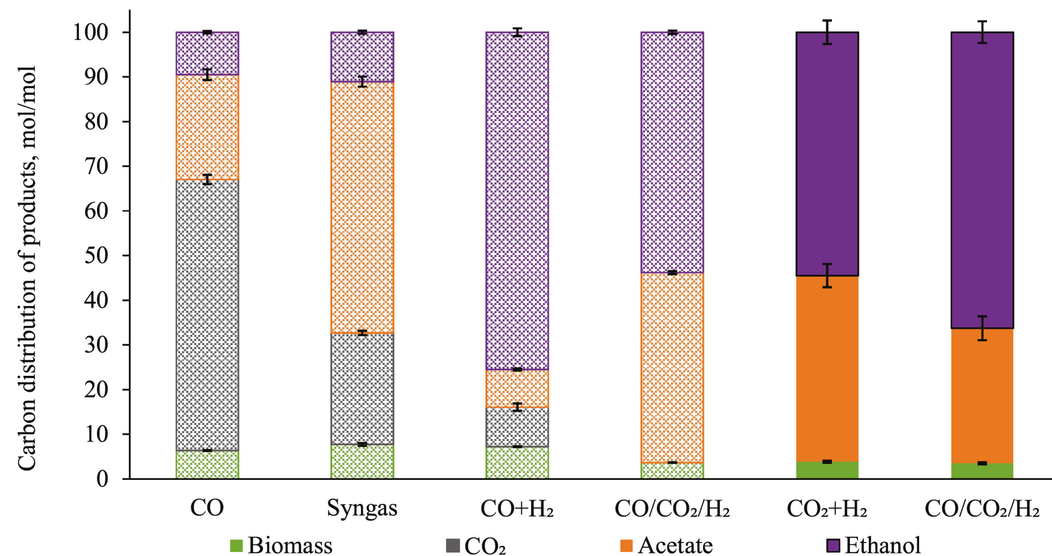
Carbon distribution of products, mol/mol
CO
Syngas
CO+H₂
CO/CO₂/H₂
CO₂+H₂
CO/CO₂/H₂
Biomass
CO₂
Acetate
Ethanol

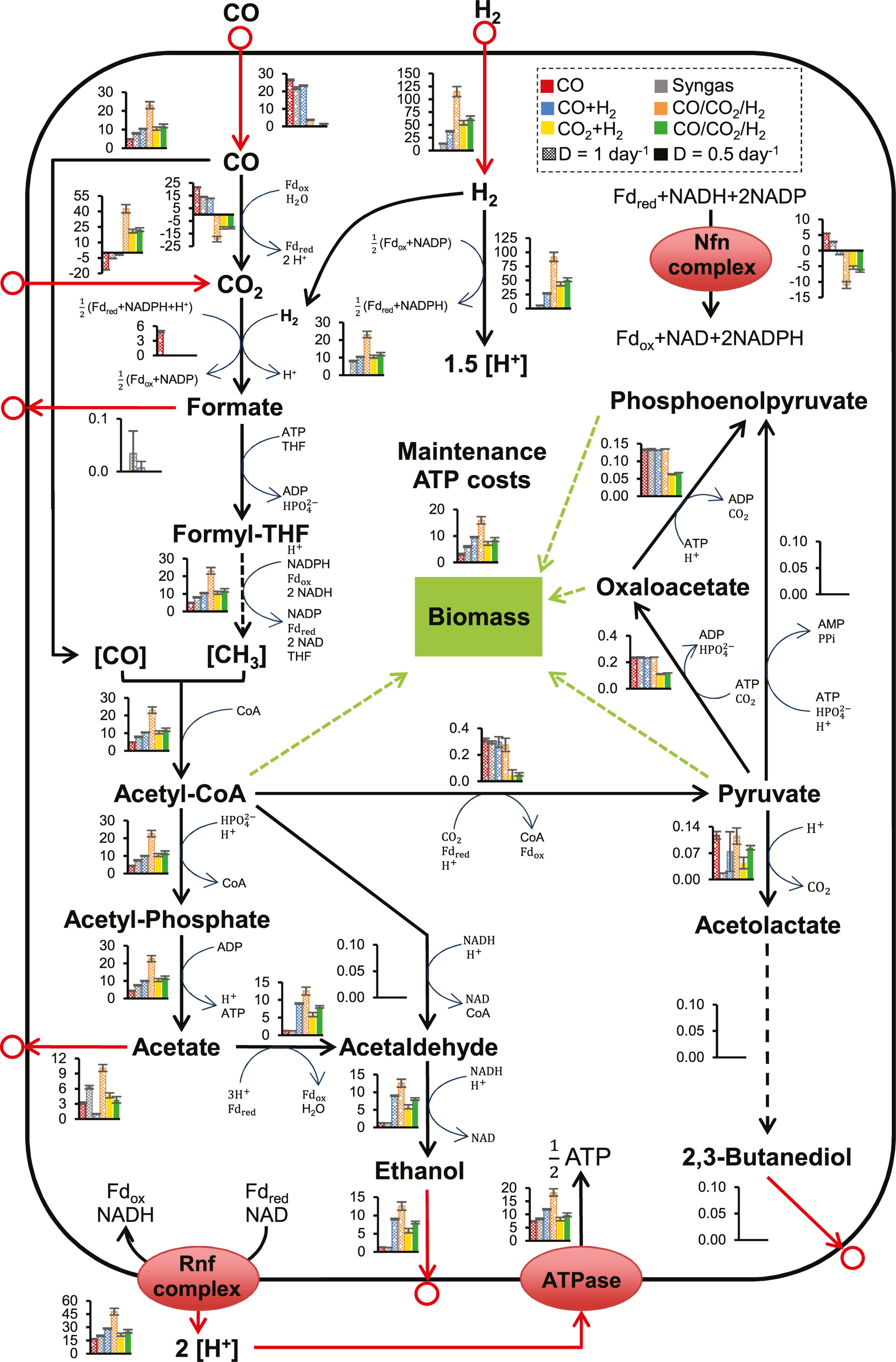

CO
H2
CO
Syngas
CO+H2
CO/CO2/H2
CO2+H2
CO/CO2/H2
D = 1 day-1
D = 0.5 day-1
CO
Fdox
H2O
Fdred
2 H+
H2
1/2 (Fdox+NADP)
1/2 (Fdred+NADPH)
1.5 [H+]
Fdred+NADH+2NADP
Nfn complex
Fdox+NAD+2NADPH
CO2
1/2 (Fdred+NADPH+H+)
H2
1/2 (Fdox+NADP)
H+
Formate
ATP
THF
ADP
HPO4 2−
Formyl-THF
H+
NADPH
Fdox
2 NADH
NADP
Fdred
2 NAD
THF
[CO]
[CH3]
CoA
Maintenance ATP costs
Biomass
Phosphoenolpyruvate
ADP
CO2
ATP
H+
Oxaloacetate
ADP
HPO4 2−
ATP
CO2
AMP
PPi
ATP
HPO4 2−
H+
Acetyl-CoA
CO2
Fdred
H+
CoA
Fdox
Pyruvate
H+
CO2
Acetolactate
HPO4 2−
H+
CoA
Acetyl-Phosphate
ADP
H+
ATP
NADH
H+
NAD
CoA
Acetate
Acetaldehyde
3H+
Fdred
Fdox
H2O
NADH
H+
NAD
Ethanol
2,3-Butanediol
1/2 ATP
Fdox
NADH
Fdred
NAD
Rnf complex
ATPase
2 [H+]